



The following Communications have been judged by at least two referees to be “very important papers” and will be published online at [www.angewandte.org](http://www.angewandte.org) soon:

X. Lou, G. Zhang, I. Herrera, R. Kinach, O. Ornatsky, V. Baranov\*,  
M. Nitz\*, M. A. Winnik\*

#### Polymer-Based Elemental Tags for Sensitive Bioassays

Y. Sawada, K. Matsumoto, T. Katsuki\*

#### Titanium-Catalyzed Asymmetric Epoxidation of Nonactivated Olefins with Hydrogen Peroxide

Z. Chen, M. Waje, W. Li, Y. Yan\*

#### Supportless Pt and PtPd Nanotubes as Electrocatalysts for Oxygen Reduction Reactions

L. Alaerts, C. E. A. Kirschhock, M. Maes, M. A. van der Veen, V. Finsy,  
A. Depla, J. A. Martens, G. V. Baron, P. A. Jacobs, J. F. M. Denayer,  
D. E. De Vos\*

#### Selective Adsorption and Separation of Xylene Isomers and Ethylbenzene with the Microporous Vanadium(IV) Terephthalate MIL-47

M. Movassaghi\*, M. A. Schmidt

#### Concise Total Synthesis of (-)-Calycanthine, (+)-Chimonanthine, and (+)-Folicanthine

Yoshihiko Ito (1937–2006)

## Obituary

M. Murakami \_\_\_\_\_ 3176

Functional Coatings by Polymer  
Microencapsulation

Swapan Kumar Ghosh

## Books

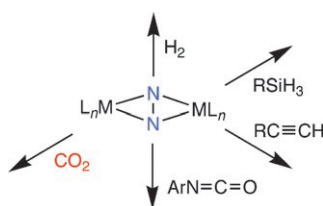
reviewed by A. F. Routh \_\_\_\_\_ 3177

Metallotherapeutic Drugs and Metal-  
Based Diagnostic Agents

Marcel Gielen, Edward R. T. Tiekink

reviewed by J. M. Zaleski \_\_\_\_\_ 3177

**Side-on matters:** When dinitrogen bridges two Group 4 metal centers in the side-on binding mode, the reactivity of the  $N_2$  unit is enhanced, as evidenced by unprecedented reactions with  $H_2$ , alkynes, silanes, isocyanates, and now carbon dioxide (see scheme). This Highlight summarizes a number of recent breakthroughs in dinitrogen functionalization by bimetallic Group 4 complexes, culminating with the reaction of  $CO_2$  with a dihafium dinitrogen derivative.



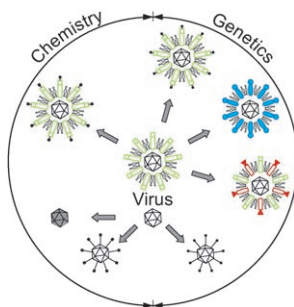
## Highlights

### Dinitrogen Functionalization

Y. Ohki, M. D. Fryzuk\* \_\_\_\_\_ 3180–3183

Dinitrogen Activation by Group 4 Metal Complexes

**Useful agents:** Viruses as nanoparticles of biological origin offer great opportunities for the design of novel materials. Precise control of their surface chemistry, together with the possibility of genetically engineering the inbuilt genome, turns viruses into a unique tool for the fabrication of multifunctional materials and devices.



## Minireviews

### Nanomaterials

M. Fischlechner, E. Donath\* \_\_\_\_\_ 3184–3193

Viruses as Building Blocks for Materials and Devices

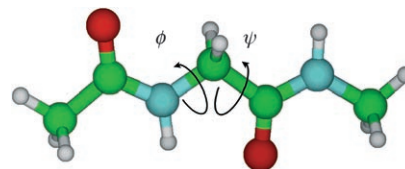
## Reviews

### Charge Transfer

E. W. Schlag,\* S.-Y. Sheu, D.-Y. Yang,  
H. L. Selzle, S. H. Lin — 3196–3210

Distal Charge Transport in Peptides

**Far-reaching consequences:** Charge transfer in peptides and proteins often leads to reactivity at a distal point. This process involves very fast facile molecular motions on a time scale of 100 fs, which is unique to peptides. The principal motions are found to be the dihedral motions between neighboring amino acids around the Ramachandran angles ( $\psi$  and  $\phi$  in the model peptide; green C, gray H, blue N, red O).

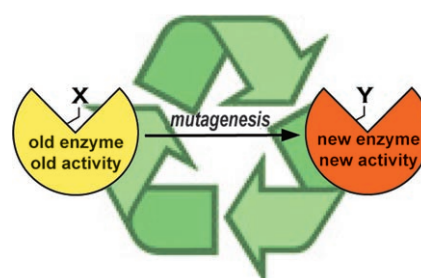


### Enzyme Design

M. D. Toscano, K. J. Woycechowsky,  
D. Hilvert\* — 3212–3236

Minimalist Active-Site Redesign: Teaching Old Enzymes New Tricks

**Reduce, reuse, recycle:** Enzymes catalyze a wide variety of chemical reactions. However, suitable enzymatic catalysts are lacking for many useful transformations. New catalytic activities arise from mutations in the active site, suggesting that the pool of existing enzymes can be a promising starting point for the creation of catalysts for nonbiological reactions. Often, a single point mutation is sufficient to endow an enzyme with a new function.



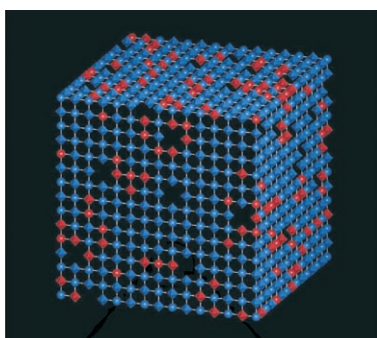
## Communications

### Magnetic Materials

S. Ohkoshi,\* H. Tokoro, T. Matsuda,  
H. Takahashi, H. Irie,  
K. Hashimoto — 3238–3241



Coexistence of Ferroelectricity and Ferromagnetism in a Rubidium Manganese Hexacyanoferrate



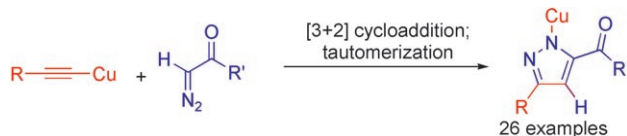
**Multiferroic material:**  $\text{Rb}^{I}_{0.82}\text{Mn}^{II}_{0.20}\text{Mn}^{III}_{0.80}[\text{Fe}^{II}(\text{CN})_6]_{0.80}[\text{Fe}^{III}(\text{CN})_6]_{0.14}\cdot\text{H}_2\text{O}$  (see picture;  $\text{Mn}^{II}$  red octahedra,  $\text{Fe}^{III}$  red spheres,  $\text{Mn}^{III}$  blue octahedra,  $\text{Fe}^{II}$  blue spheres, CN white lines, gaps are Fe vacancies;  $\text{H}_2\text{O}$  omitted) displays both ferroelectricity, explained by a mixing of  $\text{Fe}^{II}$ ,  $\text{Fe}^{III}$ , Fe vacancies,  $\text{Mn}^{II}$ , and Jahn–Teller-distorted  $\text{Mn}^{III}$  centers, and ferromagnetism, caused by a parallel ordering of the magnetic spins of  $\text{Mn}^{III}$ .

### For the USA and Canada:

ANGEWANDTE CHEMIE International Edition (ISSN 1433-7851) is published weekly by Wiley-VCH, PO Box 191161, 69451 Weinheim, Germany. Air freight and mailing in the USA by Publications Expediting Inc., 200

Meacham Ave., Elmont, NY 11003. Periodicals postage paid at Jamaica, NY 11431. US POSTMASTER: send address changes to *Angewandte Chemie*, Wiley-VCH, 111 River Street, Hoboken, NJ 07030. Annual subscription price for institutions: US\$ 5685/5168 (valid for print and

electronic / print or electronic delivery); for individuals who are personal members of a national chemical society prices are available on request. Postage and handling charges included. All prices are subject to local VAT/sales tax.



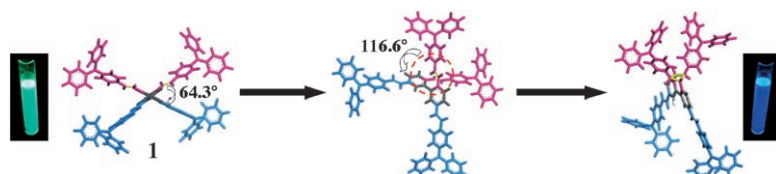
**HOMO-logous:** The copper-mediated cycloaddition of alkynes with diazo carbonyl compounds to give pyrazoles is reminiscent of the copper-catalyzed cycloaddition of alkynes and azides. The formation of the copper acetylide is

proposed to narrow the energy gap between the highest occupied molecular orbital (HOMO) of the alkyne and the lowest unoccupied molecular orbital (LUMO) of the diazo compound.

## Dipolar Cycloaddition Reactions

X. Qi, J. M. Ready\* 3242–3244

Copper-Promoted Cycloaddition of Diazocarbonyl Compounds and Acetylenes



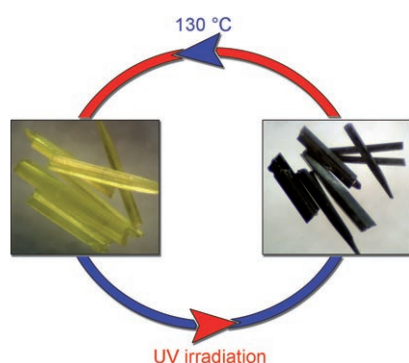
**Extremely mild conditions** are required for an intramolecular thermal [2+2] cycloaddition in the swivel-cruciform molecule **1**. As a result of the relatively free rotation about the biphenyl bond in **1** (see picture, left) a conformation is accessible in which

the alkene bonds of the two *ortho* substituents are brought into proximity in the required orthogonal arrangement, and the intramolecular cycloadduct (right) is formed at room temperature.

## Intramolecular Cycloaddition

L. Tian, F. He, H. Zhang, H. Xu, B. Yang, C. Wang, P. Lu, M. Hanif, F. Li, Y. Ma,\* J. Shen 3245–3248

Thermal Cycloaddition Facilitated by Orthogonal  $\pi$ - $\pi$  Organization through Conformational Transfer in a Swivel-Cruciform Oligo(phenylenevinylene)

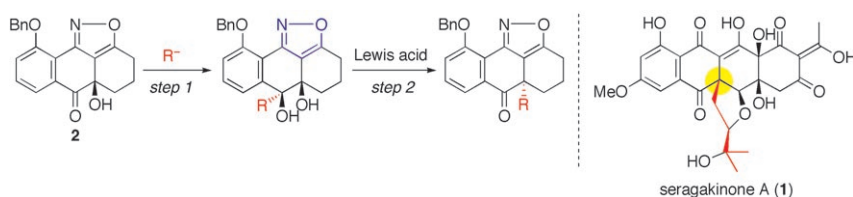


**Color scheme:** Reversibly photochromic crystals of (MV)Bi<sub>2</sub>Cl<sub>8</sub> (methyl viologen, MV<sup>2+</sup>: *N,N'*-dimethyl-4,4'-bipyridinium) show structural variations before and after UV irradiation. Color reversion is accomplished by heating in air (see picture). ([Bi<sub>2</sub>Cl<sub>8</sub>)<sub>2</sub><sup>2-</sup> double-octahedral chains serve as electron donors to in situ generated MV<sup>2+</sup> dications.

## Photochromic Crystals

G. Xu, G.-C. Guo,\* M.-S. Wang, Z.-J. Zhang, W.-T. Chen, J.-S. Huang 3249–3251

Photochromism of a Methyl Viologen Bismuth(III) Chloride: Structural Variation Before and After UV Irradiation



**Underappreciated and neglected,** isoxazoles are extremely good at stabilizing  $\alpha$  cations. This ability is exploited in a method for the stereocontrolled introduction of angular substituents as found in polyketide-derived polycyclic natural

products, such as **1**. In a two-step process, the stereoselective addition of a nucleophile to the ketone **2** is followed by a regio- and stereospecific pinacol rearrangement. Bn = benzyl; R = allyl, aryl, heteroaryl, vinyl.

## Asymmetric Synthesis

K. Suzuki,\* H. Takikawa, Y. Hachisu, J. W. Bode 3252–3254

Isoxazole-Directed Pinacol Rearrangement: Stereocontrolled Approach to Angular Stereogenic Centers





# For a Professional Touch

NALIZED • POPULAR • FAST • PERSONALIZED • POPULA

- Reprints of your Article
- High-Resolution PDF
- Personalized Reprints – for example, a bound volume of all your Wiley-VCH articles
  - with your company logo and your advertisement



## REPRINTS - YOUR TICKET TO SUCCESS!

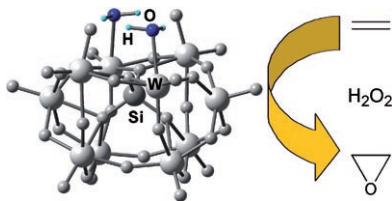
- TO ORDER AT ANY TIME!

 **WILEY-VCH**

 [www.wiley-vch.de](http://www.wiley-vch.de)

Please contact: Carmen Leitner  
Chem-reprints@wiley-vch.de





**Water in the lagoon:** A fast catalytic epoxidation of both terminal and internal double bonds was promoted by the regioselective tetraprotonation of the polyoxometalate  $\gamma\text{-(SiO}_4\text{)W}_{10}\text{O}_{32}]^{8-}$  (see picture), which leads to the localization of two water molecules on the reactive lacunary site. This mechanism was supported by evidence from kinetic, spectroscopic, and computational studies.

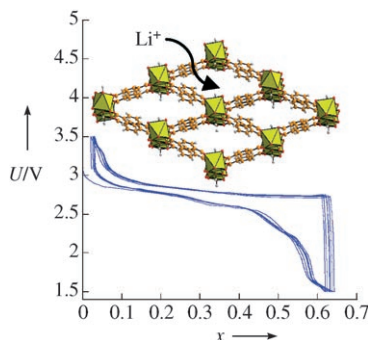
### Polyoxometalates

A. Sartorel,\* M. Carraro, A. Bagno, G. Scorrano, M. Bonchio\* — **3255–3258**

Asymmetric Tetraprotonation of  $\gamma\text{-(SiO}_4\text{)W}_{10}\text{O}_{32}]^{8-}$  Triggers a Catalytic Epoxidation Reaction: Perspectives in the Assignment of the Active Catalyst



**There's more to LiFe:** When used as an electrode in a lithium half cell, the metal-organic framework  $[\text{Li}_x\text{Fe}^{\text{II}}_x\text{Fe}^{\text{III}}_{1-x}(\text{OH})_{0.8}\text{F}_{0.2}\text{L}]$  ( $\text{L} = \text{O}_2\text{CC}_6\text{H}_4\text{CO}_2$ ) shows a reversible redox process around 3.0 V versus  $\text{Li}^+/\text{Li}^0$  with interesting capacity retention and rate capability (see voltage profile for a  $[\text{Li}_x\text{Fe}(\text{OH})_{0.8}\text{F}_{0.2}\text{L}]$  half cell; inset: representation of lithium insertion upon oxidation to  $\text{Li}^+$ ).



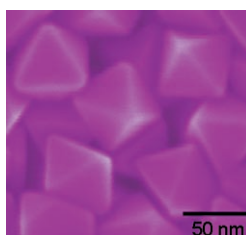
### Microporous Materials

G. Férey, F. Millange, M. Morcrette, C. Serre, M.-L. Doublet, J.-M. Grenèche, J.-M. Tarascon\* — **3259–3263**

Mixed-Valence Li/Fe-Based Metal-Organic Frameworks with Both Reversible Redox and Sorption Properties



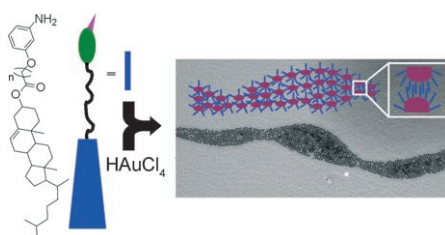
**Pieces of eight:** Single-crystalline Au nano-octahedra with well-defined shape and tunable size can be synthesized by a modified polyol process. The octahedral Au nanocrystals have sharp corners and display optical properties that are sensitive to the crystal sizes and the truncation of the tips.



### Nanocrystals

C. Li, K. L. Shuford, Q.-H. Park, W. Cai, Y. Li, E. J. Lee, S. O. Cho\* — **3264–3268**

High-Yield Synthesis of Single-Crystalline Gold Nano-octahedra



**Going through a phase:** By using simple glass-forming liquid crystals (LCs) in situ, gold nanoparticles (GNPs) were synthesized shape selectively and assembled spontaneously to generate ribbonlike

patterns that are replicas of native LC organizations. This remarkable approach afforded boomerang- and V-shaped GNPs.

### Liquid Crystals

V. A. Mallia, P. K. Vemula, G. John,\* A. Kumar, P. M. Ajayan\* — **3269–3274**

In Situ Synthesis and Assembly of Gold Nanoparticles Embedded in Glass-Forming Liquid Crystals

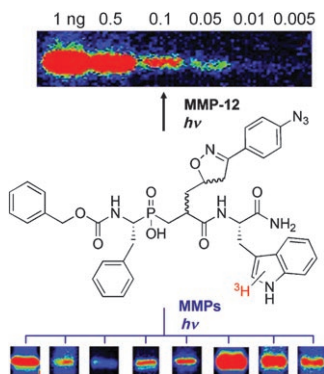


## Functional Proteomics

A. David, D. Steer, S. Bregant, L. Devel,  
A. Makaritis, F. Beau, A. Yiotakis,  
V. Dive\* 3275–3277



Cross-Linking Yield Variation of a Potent  
Matrix Metalloproteinase Photoaffinity  
Probe and Consequences for Functional  
Proteomics



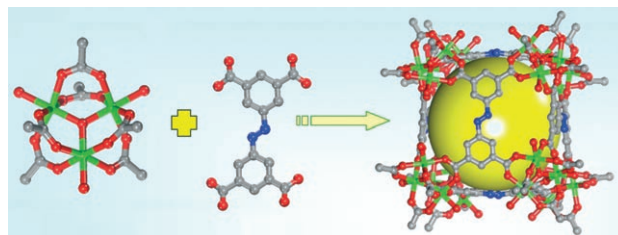
**Probing proteinases:** A radioactive photoaffinity probe exhibiting subnanomolar potency towards matrix metalloproteinases (MMPs) has been developed (see structure). High sensitivity in the detection of particular MMPs has been obtained; however, high variation in the cross-linking yield of MMPs with this probe may limit its ability to detect all MMP active forms in biological samples. This result suggests that a cocktail of optimized probes should be developed.

## Hydrogen Storage

Y. Liu, J. F. Eubank, A. J. Cairns, J. Eckert,  
V. C. Kravtsov, R. Luebke,  
M. Eddaoudi\* 3278–3283



Assembly of Metal–Organic Frameworks  
(MOFs) Based on Indium-Trimer Building  
Blocks: A Porous MOF with soc Topology  
and High Hydrogen Storage



**The key to soc-cess:** The trimer building block  $[\text{In}_3\text{O}(\text{CO}_2)_6]$  and a tetracarboxylate organic linker assemble into a novel porous metal–organic framework (see

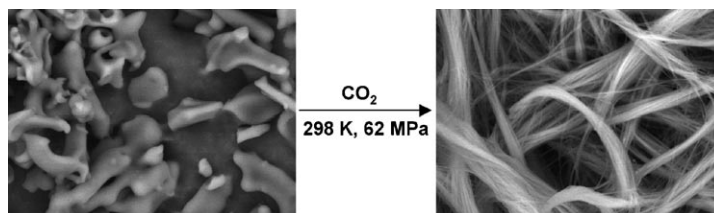
picture; In green, C gray, N blue, O red; cavity: yellow sphere) having an unprecedented soc topology (soc = square–octahedron) and high  $\text{H}_2$  uptake.

## Microfibrillar Foams

I. H. Paik, D. Tapriyal, R. M. Enick,\*  
A. D. Hamilton\* 3284–3287



Fiber Formation by Highly  $\text{CO}_2$ -Soluble  
Bisureas Containing Peracetylated  
Carbohydrate Groups



**Like dissolves like:** Bisureas containing environmentally benign  $\text{CO}_2$ -philic groups derived from peracetylated gluconic acid dissolve in supercritical  $\text{CO}_2$  at 298 K and

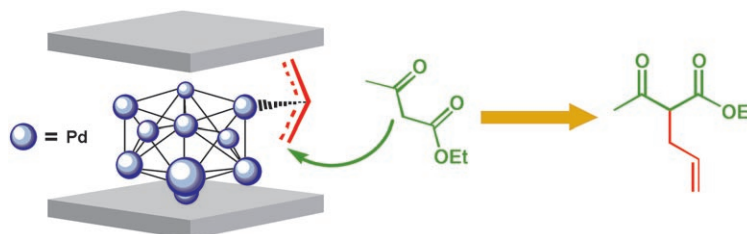
62 MPa. Upon depressurization of the  $\text{CO}_2$ , the initially powdery bisureas (left image) form microfibrillar foams (right image).

## Heterogeneous Catalysis

T. Mitsudome, K. Nose, K. Mori,  
T. Mizugaki, K. Ebitani, K. Jitsukawa,  
K. Kaneda\* 3288–3290

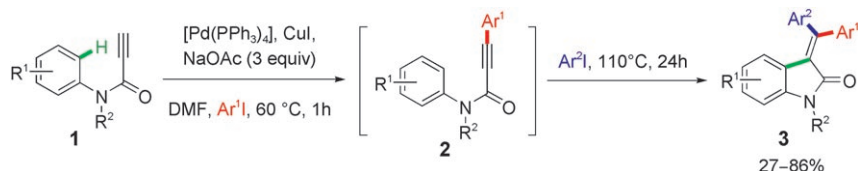


Montmorillonite-Entrapped Sub-  
nanoordered Pd Clusters as a  
Heterogeneous Catalyst for Allylic  
Substitution Reactions



**Caught making a change:** Stable sub-nanoordered Pd clusters within the interlayer spaces of montmorillonite efficiently catalyze heterogeneous allylic substitution reactions in which the coor-

dinatively unsaturated Pd atoms enable facile formation of  $\pi$ -allylpalladium intermediates (see scheme). The catalyst is reusable without any loss of activity or selectivity.



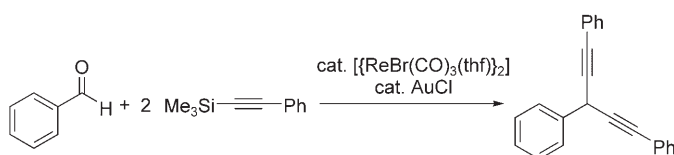
**3-3-1 Formation:**  $[\text{Pd}(\text{PPh}_3)_4]/\text{CuI}$  serves as an efficient catalyst for the reaction of three readily available starting materials to give 3-(diarylmethylene)indolin-2-ones **3** through a sequence of intermolecular Sonagashira reaction/intermolecular car-

bopalladation/C–H activation/C–C bond formation (see scheme). Three C–C bonds are thereby formed as a result of three distinct catalytic cycles with one catalyst. DMF = *N,N*-dimethylformamide.

## Domino Reactions

A. Pinto, L. Neuville, J. Zhu\* **3291–3295**

Palladium-Catalyzed Three-Component Synthesis of 3-(Diarylmethylene)oxindoles through a Domino Sonagashira/Carbopalladation/C–H Activation/C–C Bond-Forming Sequence



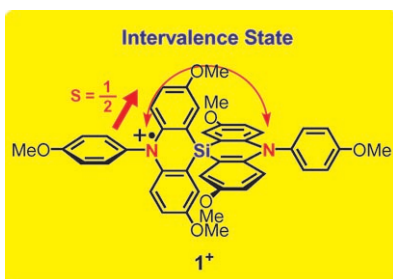
**Very couply!** Coupling reactions of propargyl or benzyl alcohols with allyl- or alkynylsilanes proceed efficiently using  $[\{\text{ReBr}(\text{CO})_3(\text{thf})\}_2]$  as catalyst. Additionally, diethynylmethane derivatives were

obtained by the reaction of aromatic aldehydes with trimethyl(phenylethynyl)silane in the presence of both the rhenium complex and AuCl (see scheme).

## Cross-Coupling

Y. Kuninobu,\* E. Ishii, K. Takai\* **3296–3299**

Rhenium- and Gold-Catalyzed Coupling of Aromatic Aldehydes with Trimethyl(phenylethynyl)silane: Synthesis of Diethynylmethanes

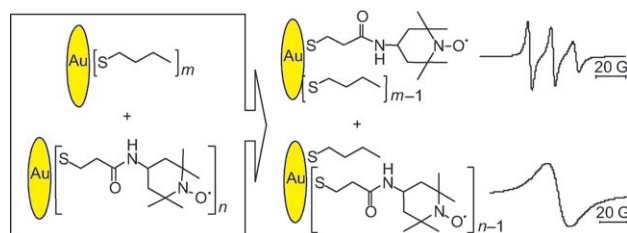


**Intriguing electronic properties** were observed for the radical cation  $1^+$  of a spiro-fused bis(triarylamine). In a new example of intramolecular spin transfer (IST) in organic intervalence systems connected by a non- $\pi$ -conjugated bridging unit, the as-prepared radical cation  $1^+$  exhibited thermally activated IST. Furthermore, it was found that  $1^+$  decomposes slowly to the tri-*p*-anisylamine radical cation.

## Molecular Electronics

Y. Hirao, M. Urabe, A. Ito,\* K. Tanaka\* **3300–3303**

Intramolecular Spin Transfer in a Spiro-Fused Bis(triarylamine)



**Jump up and down:** EPR spectroscopy was used to monitor hopping of spin-labeled ligands between Au nanoparticles. The slow interparticle exchange affects approximately 20% of the binding sites on

the nanoparticle surface. The kinetic analysis showed that this reaction follows a dissociative mechanism with ligand desorption in the rate-determining step. EPR = electron paramagnetic resonance.

## Ligand Exchange

M. Zachary, V. Chechik\* **3304–3307**

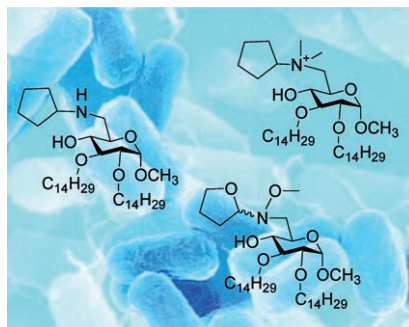
Hopping of Thiolate Ligands between Au Nanoparticles Revealed by EPR Spectroscopy

## Drug Discovery

F. Peri,\* F. Granucci, B. Costa, I. Zanoni,  
C. Marinzi, F. Nicotra — 3308–3312



Inhibition of Lipid A Stimulated Activation of Human Dendritic Cells and Macrophages by Amino and Hydroxylamino Monosaccharides



**Innovative mimics** of lipid A were synthesized and shown to efficiently inhibit lipid A induced cytokine production in human dendritic cells and macrophages. These compounds, which consist of a D-glucose unit functionalized with an amine, ammonium, or hydroxylamine group and a five-membered ring at C6 (see structures) are promising leads for antiseptic drug development owing to their lack of toxicity and their selectivity for the TLR4 receptor.

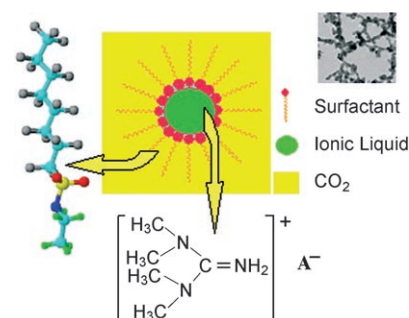
## Micelles

J. Liu, S. Cheng, J. Zhang, X. Feng, X. Fu,  
B. Han\* — 3313–3315



Reverse Micelles in Carbon Dioxide with Ionic-Liquid Domains

The fluorinated surfactant *N*-ethyl perfluorooctylsulfonamide can form reverse micelles with an ionic liquid as the inner component in supercritical CO<sub>2</sub>. These reverse micelles can solubilize salts and gold nanoparticles can be formed with HAuCl<sub>4</sub> (see TEM image). The micellar systems may combine some of the advantages of supercritical CO<sub>2</sub> and ionic liquids as solvents with benefits for potential applications.

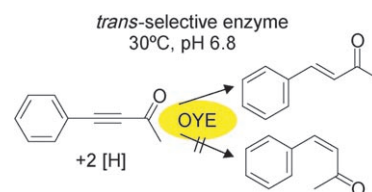


## Enzyme Catalysis

A. Müller, R. Stürmer, B. Hauer,  
B. Rosche\* — 3316–3318

Stereospecific Alkyne Reduction: Novel Activity of Old Yellow Enzymes

**Old enzyme, new trick:** An environmentally sustainable alternative for the regio- and stereoselective reduction of the alkyne bond is the biotransformation by “Old Yellow Enzyme” (OYE). This “old” enzyme, first isolated in 1932, catalyzes the *trans*-selective hydrogenation of the carbon–carbon triple bond under mild conditions.

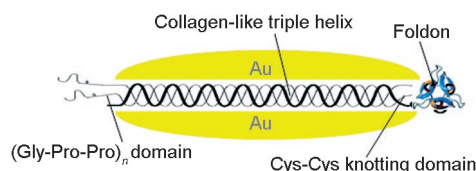


## Biomolecular Nanowires

H. Bai, K. Xu, Y. Xu,\*  
H. Matsui\* — 3319–3322



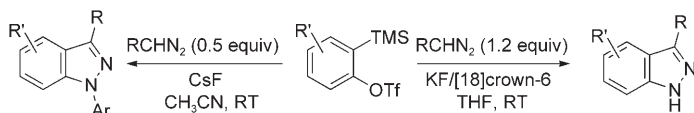
Fabrication of Au Nanowires of Uniform Length and Diameter Using a Monodisperse and Rigid Biomolecular Template: Collagen-like Triple Helix



**Collagen implants:** The unique molecular properties of the collagen-like triple helix, generated and amplified by recombinant technology, enable the formation of rigid rod-shaped molecules that are ideally

suited as biomolecular-nanowire templates. Biomineralization of Au on the triple helix (see picture) produces monodisperse Au nanowires with dimensions 4x40 nm<sup>2</sup>.





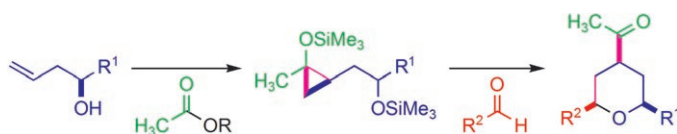
**Take your pick:** Both N-unsubstituted and 1-aryl 1*H*-indazoles are available in good to high yields through the [3+2] cycloaddition of benzynes derived from *o*-silylaryl triflates with diazomethane

derivatives (see scheme). In the presence of KF/[18]crown-6, the N-unsubstituted 1*H*-indazole is formed, whereas the 1-arylated product is obtained regioselectively with CsF and an excess of the triflate.

## Synthesis of Heterocycles

T. Jin, Y. Yamamoto\* 3323–3325

An Efficient, Facile, and General Synthesis of 1*H*-Indazoles by 1,3-Dipolar Cycloaddition of Benzynes with Diazomethane Derivatives



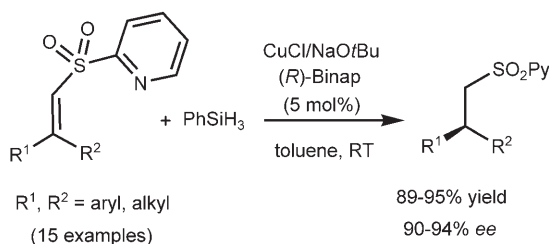
**A convenient method** for preparing all-*cis* 2,4,6-trisubstituted tetrahydropyrans and the corresponding 2,6-*trans* isomers has been developed. This trimethylsilyl triflate mediated coupling of cyclopropanols with

a 2-hydroxyalkyl side chain to aldehydes (see scheme) is also suitable for the coupling of two large subunits to generate structural complexity in a rapid and highly convergent manner.

## Cyclic Ethers

H. G. Lee, I. L. Lysenko, J. K. Cha\* 3326–3328

Stereoselective Synthesis of 2,4,6-Trisubstituted Tetrahydropyrans by the Use of Cyclopropanols as Homoenols



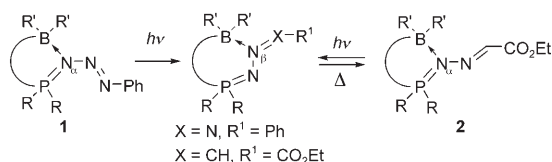
**Access to a chiral sulfone:** Asymmetric conjugate reduction of  $\beta,\beta$ -disubstituted  $\alpha,\beta$ -unsaturated 2-pyridylsulfones with silanes under Cu<sup>I</sup>/binap catalysis provides chiral sulfones with excellent chemical yields and enantioselectivities (see

scheme). These enantioenriched 2-pyridylsulfones are versatile intermediates in the preparation of a wide variety of functionalized chiral compounds. binap = 2,2'-bis(diphenylphosphanyl)-1,1'-binaphthyl.

## Asymmetric Catalysis

T. Llamas, R. G. Arrayás, J. C. Carretero\* 3329–3332

Catalytic Asymmetric Conjugate Reduction of  $\beta,\beta$ -Disubstituted  $\alpha,\beta$ -Unsaturated Sulfones



**Stable relations:** Reaction of phenylazide with a phosphine borane derivative gives rise to an intramolecularly stabilized phosphazide **1** ( $R = iPr$ ,  $R' = \text{mesityl}$ ) that undergoes an unprecedented photoisomerization process associated with a

change from an  $N_\alpha \rightarrow B$  to an  $N_\beta \rightarrow B$  interaction (see scheme). The generality and possible reversibility of such phenomena are demonstrated with the related phosphazine adduct **2**.

## Phosphorus Heterocycles

M. W. P. Bebbington, S. Bontemps, G. Bouhadir, D. Bourissou\* 3333–3336

Photoisomerizable Heterodienes Derived from a Phosphine Borane

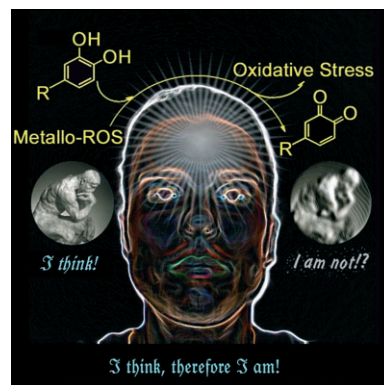
## Alzheimer's Disease

G. F. Z. da Silva, L.-J. Ming\* 3337–3341



Metallo-ROS in Alzheimer's Disease: Oxidation of Neurotransmitters by Cu<sup>II</sup>-β-Amyloid and Neuropathology of the Disease

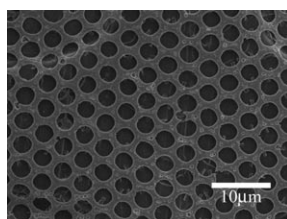
**A clear mind:** The Cu<sup>II</sup>-β-amyloid (Aβ) complex has been shown to exhibit enzyme-like metal-centered oxidative and hydroxylation catalyses. Metal-centered oxidation of various neurotransmitters by CuAβ under biomimetic conditions has verified the bio-relevance of the metal-centered catalyses and is expected to provide a chemical basis for the better understanding of the etiology of Alzheimer's disease. ROS = reactive oxygen species.



## Polyoxometalates

D. Fan, X. Jia, P. Tang, J. Hao,\*  
T. Liu\* 3342–3345

Self-Patterning of Hydrophobic Materials into Highly Ordered Honeycomb Nanostructures at the Air/Water Interface

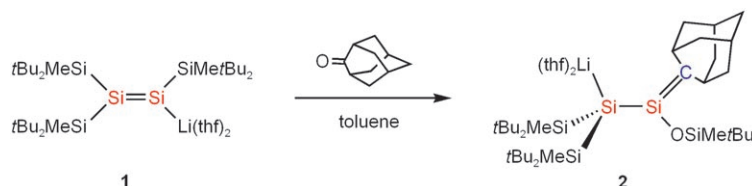


**Patterns of behavior:** Complexes of the cluster {Mo<sub>72</sub>Fe<sub>30</sub>} and the surfactant dioctadecyldimethylammonium chloride (DODMACl) produced in CHCl<sub>3</sub> form patterns with a honeycomb structure at the air/water interface after evaporation of the solvent (see SEM image). The concentration of DODMACl in CHCl<sub>3</sub> is critical to whether the {Mo<sub>72</sub>Fe<sub>30</sub>} macroanions remain in the aqueous or CHCl<sub>3</sub> phase.

## Silene Derivatives

S. Inoue, M. Ichinohe,  
A. Sekiguchi\* 3346–3348

Conversion of a Disilenide into a Silene: Silyl-Anion-Substituted Silene by a Sila-Peterson-Type Reaction from an sp<sup>2</sup>-Type Silyl Anion



**From Si=Si to Si=C:** Silyl-anion-substituted silene **2** was synthesized as air- and moisture-sensitive yellow crystals by the reaction of the disilenyl lithium derivative **1** with adamantanone (see scheme). The

physical properties of **2** suggest a silene-type structure containing a silicon–carbon double bond, with no contribution from 1,2-disilaallyl-anion-type and disilene-type structures.

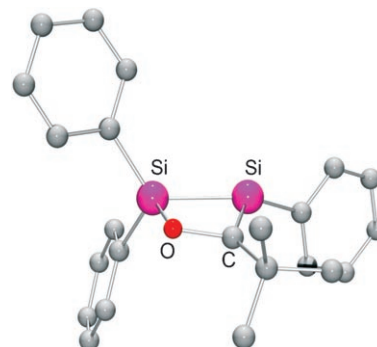
## Si=C Bonds

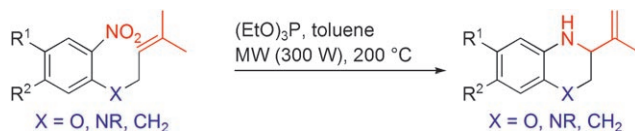
I. Bejan, D. Güclü, S. Inoue, M. Ichinohe,  
A. Sekiguchi,  
D. Scheschkewitz\* 3349–3352



Stable Cyclic Silenes from Reaction of Disilenides with Carboxylic Acid Chlorides

**Pyramidal silicon centers** within the Si=C bond are the most prominent feature of the first cyclic silenes stable at room temperature, as exhibited by X-ray diffraction (see structure) and calculations. They are quantitatively formed by reaction of lithium disilenides, disila analogues of vinyl lithium compounds, with acid chlorides, and are relatively inert, for example, towards the addition of MeOH.





**Domino on cycles:** Several N-heterocycles, such as 3,4-dihydro-2H-1,4-benzoxazines, 1,2,3,4-tetrahydroquinoxalines, and 1,2,3,4-tetrahydroquinolines, can be obtained through a novel domino reaction

mediated by triethyl phosphite under the influence of microwave irradiation (MW) in a single step from nitroaromatic compounds (see scheme).

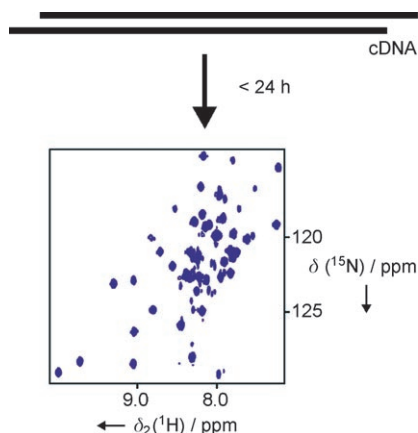
### Domino reactions

E. Merişor, J. Conrad, I. Klaiber, S. Mika, U. Beifuss\* 3353–3355

Triethyl Phosphite Mediated Domino Reaction: Direct Conversion of  $\omega$ -Nitroalkenes Into N-Heterocycles



**Quick and clean:** Excellent protein yields in cell-free protein synthesis can be obtained by using polymerase chain reaction (PCR) amplified DNA templates, provided that the templates are designed for cyclization. This eliminates time-consuming cloning steps and allows one to go from complementary DNA to the protein NMR spectrum in 24 h.



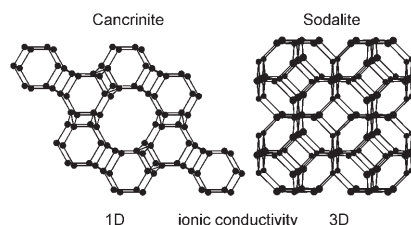
### Protein Production

P. S. C. Wu, K. Ozawa, S. P. Lim, S. G. Vasudevan, N. E. Dixon, G. Otting\* 3356–3358

Cell-Free Transcription/Translation from PCR-Amplified DNA for High-Throughput NMR Studies



**Different cation conduction mechanisms** in the zeolites cancrinite and sodalite were revealed by the combination of impedance and solid-state NMR spectroscopies. Cancrinite is a one-dimensional conductor as a result of its channels, which are made up of stacked 12-rings, whereas the cation transport in sodalite takes place in three dimensions.

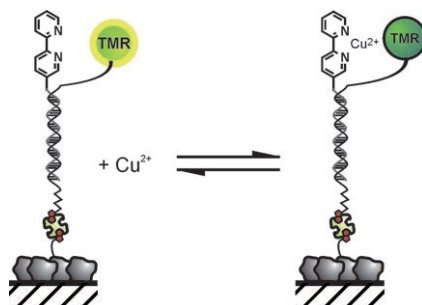


### Ion Transport in Zeolites

E. Jordan, D. Wilmer, H. Koller\* 3359–3362

Matrix Effect on Motional Coupling and Long-Range Transport of Cations in Zeolites

**For the observation of the coordination** states of individual copper(II) chelate complexes in thermodynamic equilibrium (see picture; TMR=tetramethylrhodamine), single-molecule fluorescence spectroscopy can be used. Application of time-resolved single-molecule spectroscopy opens new prospects for the investigation of reactions in the coordination sphere of metal complexes.



### Single-Molecule Studies

A. Kiel, J. Kovacs, A. Mokhir, R. Krämer, D.-P. Herten\* 3363–3366

Direct Monitoring of Formation and Dissociation of Individual Metal Complexes by Single-Molecule Fluorescence Spectroscopy



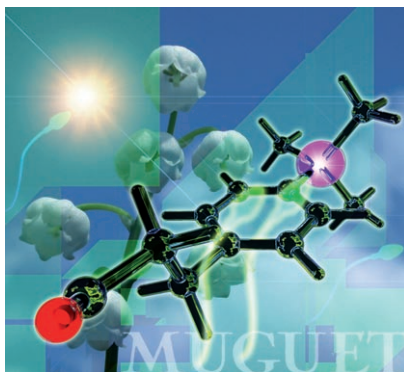


## Carbon–Silicon Exchange

L. Doszczak, P. Kraft,\* H.-P. Weber,  
R. Bertermann, A. Triller, H. Hatt,\*  
R. Tacke\* \_\_\_\_\_ 3367–3371



Prediction of Perception: Probing the hOR17-4 Olfactory Receptor Model with Silicon Analogues of Bourgeonal and Lilial



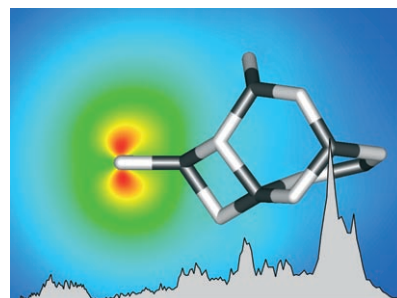
**Sense and sensibility:** Silicon analogues of the lily-of-the-valley odorants lilial and bourgeonal demonstrate that the electronic surface structure determines the interaction of an odorant with its olfactory receptor. The subtle changes in the stereoelectronic properties enable a comparison of in vivo, in vitro, and in silico data. Odor thresholds, as well as the swimming behavior of sperm cells, correlate well with the binding energies obtained from a computational model of the hOR17-4 receptor.

## Gas-Phase Clusters

M. Sierka,\* J. Döbler, J. Sauer,  
G. Santambrogio, M. Brümmer, L. Wöste,  
E. Janssens, G. Meijer,  
K. R. Asmis\* \_\_\_\_\_ 3372–3375

Unexpected Structures of Aluminum Oxide Clusters in the Gas Phase

**No family resemblance:** IR photodissociation experiments and DFT optimizations implementing a genetic algorithm suggest that small aluminum oxide clusters have unusual structures in the gas phase. For example, the structure proposed for  $[(\text{Al}_2\text{O}_3)_4]^+$  (see picture; Al black, O gray) has no features in common with bulk alumina phases.



Supporting information is available on the WWW (see article for access details).



A video clip is available as Supporting Information on the WWW (see article for access details).

## Sources

### Product and Company Directory

You can start the entry for your company in “Sources” in any issue of *Angewandte Chemie*.

If you would like more information, please do not hesitate to contact us.

Wiley-VCH Verlag – Advertising Department

Tel.: ☎ 62 01 - 60 65 65

Fax: ☎ 62 01 - 60 65 50

E-Mail: MSchulz@wiley-vch.de

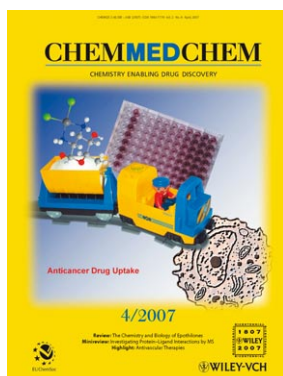
## Service

**Keywords** \_\_\_\_\_ 3376

**Authors** \_\_\_\_\_ 3377

**Angewandte's Sister Journals** \_\_\_\_\_ 3174

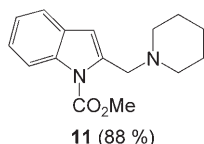
**Preview** \_\_\_\_\_ 3379



For more information on  
ChemMedChem see  
[www.chemmedchem.org](http://www.chemmedchem.org)

## Corrigendum

It has been brought to the authors attention that the chemical structure for compound **11**, shown in Table 3 in their recent Communication, was incorrectly drawn. The correct structure is shown below. The authors apologize for their oversight.



Direct Synthesis of 2-(Aminomethyl)-indoles through Copper(I)-Catalyzed Domino Three-Component Coupling and Cyclization Reactions

H. Ohno,\* Y. Ohta, S. Oishi,  
N. Fujii\* \_\_\_\_\_ **2295–2298**

*Angew. Chem. Int. Ed.* **2007**, 46

DOI 10.1002/anie.200604342



## ESOR XI

11<sup>TH</sup> EUROPEAN SYMPOSIUM ON ORGANIC REACTIVITY

11<sup>th</sup> European Symposium on Organic Reactivity,  
Universidade do Algarve, Faro, Portugal, 1. – 6. July, 2007. <http://www.ualg.pt/esorxi/>

## Confirmed Plenary Lecturers

Ben Feringa, Groningen, NL  
Cinzia Chiappe, Pisa, IT  
Colin Suckling, Strathclyde, GB  
François Diederich, Zurich, CH  
Gary Posner, Baltimore, USA  
Herbert Mayr, Munich, GE  
Jean-Marie Aubry, Lille, FR  
José Artur Martinho Simões, Lisboa, PT  
Sebastião Formosinho, Coimbra, PT  
William Jorgensen, Newhaven, USA  
Yitzhak Apeloig, Haifa, IL

## Confirmed Invited Lecturers

Addy Pross, Beer Sheva, IL  
Andrée Kirsch-De Mesmaeker, Bruxelles BE  
Gerd Kaupp, Oldenburg, GE  
Hideo Tomioka, Mie, JP  
John Richard, Buffalo, USA  
Luigi Mandolini, Roma, IT  
Manuel García Basallote, Cádiz, ES  
Rui Fausto, Coimbra, PT

Chair and contact: Maria de Lurdes Cristiano.  
Dep. Química e Bioquímica, Faculdade de  
Ciências Universidade do Algarve  
8005-139 Faro, Portugal, e-mail:ESORXI@ualg.pt